

RSC Advances



This is an *Accepted Manuscript*, which has been through the Royal Society of Chemistry peer review process and has been accepted for publication.

Accepted Manuscripts are published online shortly after acceptance, before technical editing, formatting and proof reading. Using this free service, authors can make their results available to the community, in citable form, before we publish the edited article. This *Accepted Manuscript* will be replaced by the edited, formatted and paginated article as soon as this is available.

You can find more information about *Accepted Manuscripts* in the [Information for Authors](#).

Please note that technical editing may introduce minor changes to the text and/or graphics, which may alter content. The journal's standard [Terms & Conditions](#) and the [Ethical guidelines](#) still apply. In no event shall the Royal Society of Chemistry be held responsible for any errors or omissions in this *Accepted Manuscript* or any consequences arising from the use of any information it contains.

ARTICLE

Hydrothermal synthesis of single crystal CoAs_2O_4 and NiAs_2O_4 compounds and their magnetic properties

Cite this: DOI: 10.1039/x0xx00000x

Tamara Đorđević,^{a*} Astrid Wittwer^a, Zvonko Jagličić^{b,c} and Igor Djerdj^dReceived 00th January 2012,
Accepted 00th January 2012

DOI: 10.1039/x0xx00000x

www.rsc.org/

The crystal structures of the hydrothermally synthesised trippkeite-related materials, CoAs_2O_4 and NiAs_2O_4 were investigated by means of single-crystal X-ray diffraction, Raman and infrared spectroscopy. As obtained compounds crystallise in the tetragonal crystal system ($P4_2/mbc$), with unit cell parameters at 293 K of $a = 8.34530(10) / 8.2277(12) \text{ \AA}$, $c = 5.62010(10) / 5.6120(11) \text{ \AA}$, $V = 391.406(12) / 379.90(13) \text{ \AA}^3$, $Z = 4$, for CoAs_2O_4 and NiAs_2O_4 respectively. Magnetic measurements show that the resulting single crystal of NiAs_2O_4 exhibit an antiferromagnetic transition at $T_N = 53 \text{ K}$ in high magnetic field of 10 kOe, as already reported in the literature. The single crystal of CoAs_2O_4 reveals an interplay between ferromagnetic and a canted antiferromagnetic interactions resulting in a canted antiferromagnetic state which occurs at 105 K - the highest critical temperature among all similar structures.

1. Introduction

In order to recognise the role of arsenic in the environment, one has to investigate structures and stabilities of naturally occurring arsenic compounds. Besides, a study of mineral-related synthetic phases should be supportive, because they can appear as consequence of human activities. The susceptibility of As(III) to oxidation to As(V) in oxide environments affords high thermal stability only to ternary $X\text{-As(V)-O}$ oxides ($X = \text{Mg}$ and divalent 3d transition metal) with arsenic in its higher oxidation state. However, under strict synthetic conditions, $X\text{-As(III)-O}$ oxides can be formed. For that reason, anhydrous arsenates of cobalt and nickel are well-established but arsenites of cobalt and nickel are less known. Besides $\text{Co}_2\text{As}_2\text{O}_5$ ¹, CoAs_2O_4 represents the second compound in the Co(II)-As(III)-O system and the NiAs_2O_4 is the first structurally determined compound in the Ni(II)-As(III)-O system.

CoAs_2O_4 and NiAs_2O_4 are isostructural to the $M^{2+}X^{3+}_2\text{O}_4$ materials and minerals²⁻⁹, with the exception of ZnAs_2O_4 ³. These compounds crystallise tetragonal, adopting space group $P4_2/mbc$, and contain chains of edge-linked MO_6 octahedra running along [001]; the chains are connected via trigonal pyramidal XO_3 units.

All MSb_2O_4 phases, with the exception of MgSb_2O_4 ⁴, have been shown to display antiferromagnetic ordering with Néel temperatures in the range 40–60 K and a transition of the magnetic modal ordering from a predominant A mode to a C mode (vide infra) on crossing the

first row transition metals^{5,7,8,10}. The edge sharing nature of the octahedra and the superexchange interactions between the M^{2+} transition metals in the chains and between the chains are responsible for the magnetic properties of these group compounds. However, no crystallographic and magnetic structures have been reported for the $M^{2+}\text{As}_2\text{O}_4$ ($M^{2+} = \text{Co}, \text{Ni}$) compounds. Molecular susceptibility of NiAs_2O_4 has been measured and the values of the Néel temperature and the asymptotic Curie temperature are given¹¹.

CoAs_2O_4 and NiAs_2O_4 were synthesised during an on-going research on natural and synthetic arsenic oxo-salts, with a focus on their structural and spectroscopic classification. The present article reports the hydrothermal synthesis of two new arsenites, CoAs_2O_4 and NiAs_2O_4 . The results of the determination of their crystal structures based on single-crystal X-ray diffraction data are given and the relationship to the known $M^{2+}X_2\text{O}_4$ compounds is discussed. To obtain further information on anion groups, Raman and infrared spectra were acquired. Due to the presence of transition metal M^{2+} cations, non-diamagnetic ground state of as grown crystals is expected and investigated using SQUID measurements. Continuous investigations on the crystal chemistry of the arsenic oxo-salts are performed because arsenic is at the top of the priority of the most hazardous substances, but less is known about its crystal structures.

2. Experimental

2.1 Materials

The materials used were: KCl (Loba Chemie, 13508), Co(OH)_2 (Sigma-Aldrich, 342440, tech. 95 %), $\text{Ni(NO}_3)_2$ (Sigma-Aldrich 244074-500G), As_2O_3 (Alfa Aesar 33289, ACS 99.95-100.05 %).

^a Institut für Mineralogie und Kristallographie, Universität Wien, Althanstraße 14, A-1090 Wien, Austria. E-mail: tamara.djordjevic@univie.ac.at

^b Institute of Mathematics, Physics and Mechanics, Jadranska 19, 1000, Ljubljana, Slovenia.

^c Faculty of Civil and Geodetic Engineering, University of Ljubljana, Jamova 2, 1000 Ljubljana, Slovenia.

^d Ruđer Bošković Institute, Bijenička 54, 10000 Zagreb, Croatia.

† Electronic Supplementary Information (ESI) available: CIF files of the structures. See DOI: 10.1039/b000000x/

2.1.1 Preparation of CoAs₂O₄

During an on-going research on synthetic mineral-like arsenites in the $M1-M2-As(III)-(H)-(Cl)$ system ($M1 = Na^+, K^+, Sr^{2+}, Ba^{2+}$; $M2 = Mg^{2+}, Mn^{2+,3+}, Fe^{2+,3+}, Co^{2+}, Ni^{2+}, Cu^{2+}, Zn^{2+}$), with a focus on their structural and spectroscopic classification, single crystals of CoAs₂O₄ were obtained. The crystals of CoAs₂O₄ were grown under hydrothermal conditions in Teflon-lined stainless steel autoclaves from a mixture of KCl, Co(OH)₂, As₂O₃ and distilled H₂O in molar ratio 1:1:1. The initial pH value of the mixture was 6. The stainless-steel autoclave was then closed and the crystallisation was carried out by placing the autoclave in oven under air atmosphere and heating the mixture under autogenous pressure from room temperature. A heating regime with three steps was chosen: the autoclaves were heated from 20° C to 200° C (four hours), held at 200° C for 199 h, and finally cooled to room temperature within 98 h. The pH value of supernatant solution was 6. The obtained products were washed with distilled water, filtered and dried in the air at room temperature. CoAs₂O₄ crystallised as pink transparent elongated prisms (yield 60 %) (Fig. 1a) together with transparent crystals of KAs₄O₆Cl¹² (yield 40 %). The maximal length of crystals was about 2 mm.

2.1.2 Preparation of NiAs₂O₄

After successful synthesis of the single crystals of CoAs₂O₄, systematic synthesis of the single crystals of $M^{2+}As_2O_4$ ($M = Mn, Fe, Co, Ni$) was performed. However, only attempts to get single crystals of CoAs₂O₄ and NiAs₂O₄ were fruitful. The crystals of NiAs₂O₄ were grown from a mixture of Ni(NO₃)₂, As₂O₃ and distilled H₂O in molar ratio 1:1. The initial pH value of the mixture was kept at around 2.5 in order to avoid the oxidation of As³⁺ to As⁵⁺. A heating regime with three steps was chosen: the autoclaves were heated from 20° C to 220° C (four hours), held at 220° C for 56 h, and slowly cooled to room temperature within 320 h. The pH value of supernatant solution was 4. The products obtained were washed with distilled water, filtered and dried in the air at room temperature. NiAs₂O₄ crystallised as green transparent elongated prisms (yield ca. 95 %) (Fig. 1b). The maximal length of crystals was about 1.7 mm.

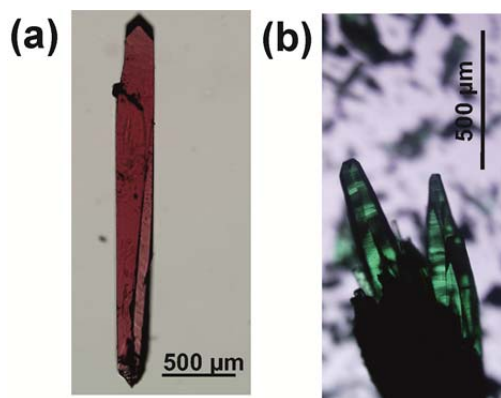


Figure 1 Single crystals of (a) CoAs₂O₄ and (b) NiAs₂O₄.

2.2 Single-crystal X-ray diffraction measurements

Several single crystals of the two title compounds were studied on a Bruker AXS Kappa APEX II CCD diffractometer, equipped with a monochromator collimator and graphite-monochromatised MoK α radiation ($\lambda = 0.71073$ Å). Single-crystal X-ray diffraction data were collected at room temperature, integrated and corrected for Lorentz and polarization factors and absorption correction by evaluation of partial multiscans (see table 1 for details). The intensity data were processed with the Bruker-Nonius programme suite SAINT-Plus¹³ and corrected for Lorentz, polarization, background and absorption effects. Their crystal structures were refined with SHELXL-97¹⁴ and WinGX¹⁵ starting from the atomic coordinates given for isotypic CuAs₂O₄².

Relevant information on crystal data, data collection, and refinements are compiled in Table 1. For final positional and displacement parameters see CIF files.† Selected bond lengths and angles for both arsenites are presented in Table 2.

Table 1 Crystal data, data collection and refinement details for CoAs₂O₄ and NiAs₂O₄

Crystal data		
Chemical formula	CoAs ₂ O ₄	NiAs ₂ O ₄
Temperature (K)	293 (2)	293 (2)
Crystal form, colour	prismatic, pink	prismatic, green
Formula weight, M_r (g mol ⁻¹)	272.77	272.55
System, space group (No.)	Tetragonal, Pa_2/mbc (135)	
a (Å)	8.34530(10)	8.2277(12)
c (Å)	5.62010(10)	5.6120(11)
V (Å ³)	391.406(12)	379.90(13)
Z	4	4
$F(000)$	500	504
Calculated density, D_x (g cm ⁻³)	4.629	4.765
Absorption coefficient, μ (mm ⁻¹)	21.032	22.258
Transmission factors, T_{min}/T_{max}	0.124/0.678	0.135/0.664
Crystal size (mm)	0.02 × 0.02 × 0.17	0.02 × 0.02 × 0.15
Reflections collected/unique	11599/838	7925/595
Observed reflections [$I > 2\sigma(I)$]	719	532
R_{int}	0.0418	0.0382
Range for data collection, θ (°)	3.452 - 44.387	3.502 - 39.118
Range of Miller indices	-15 ≤ h ≤ 16; -16 ≤ k ≤ 16; -10 ≤ l ≤ 9	-14 ≤ h ≤ 14; -8 ≤ k ≤ 12; -9 ≤ l ≤ 9
Extinction coefficient, k^a	0.0159(8)	0.0056(5)
Refined parameters	22	22
R -indices [$I > 2\sigma(I)$] ^a	$R_1 = 0.0229$ $wR_2 = 0.0440$	$R_1 = 0.0161$ $wR_2 = 0.0363$
R -indices (all data) ^a	$R_1 = 0.0306$ $wR_2 = 0.0455$	$R_1 = 0.0371$ $wR_2 = 0.059$
Goodness-of-fit, S	1.079	1.09
$(\Delta\rho)_{max}, (\Delta\rho)_{min}$ (e Å ⁻³)	1.088, -1.022	0.490, -0.656

^a $w = 1/[\sigma^2(F_o) + (0.0197P)^2 + 0.1338P]$ for CoAs₂O₄, $w = 1/[\sigma^2(F_o) + (0.0129P)^2 + 0.2839P]$ for NiAs₂O₄.

2.3 Vibrational spectroscopy measurements

The single-crystal Raman spectra and Raman spectra of the bulk material of CoAs₂O₄ and NiAs₂O₄ were collected using a Horiba LabRam HR Evolution system equipped with a Si-based, Peltier-cooled CCD detector in the spectral range from 4000 to 60 cm⁻¹. The 633 nm excitation line of a He-Ne laser was focused with a 100× objective on the randomly oriented single crystal. The sample spectra were acquired with a nominal exposure time of 5 s and 10 s, for Co- and Ni-arsenite, respectively (confocal mode, Olympus 1800 lines/mm, 1.5 µm lateral resolution, approximately 3 µm depth resolution).

Table 2 Selected bond distances (Å) and angles (°) for CoAs₂O₄ and NiAs₂O₄

CoAs ₂ O ₄		NiAs ₂ O ₄	
Co—O2	2.0305(7)	Ni—O2	2.0079(9)
—O2 ⁱ	2.0305(7)	—O2 ⁱ	2.0079(9)
—O2 ⁱⁱ	2.0305(7)	—O2 ⁱⁱ	2.0079(9)
—O2 ⁱⁱⁱ	2.0305(7)	—O2 ⁱⁱⁱ	2.0079(9)
—O1	2.1775(11)	—O1	2.1222(13)
—O1 ^{iv}	2.1775(11)	—O1 ^{iv}	2.1222(13)
<Co—O>	2.0795	<Ni—O>	2.046
As—O2 ^v	1.7292(11)	As—O2 ^v	1.7275(12)
—O1 ^{vi}	1.8473(5)	—O1 ^{vi}	1.8501(6)
—O1	1.8473(5)	—O1	1.8501(6)
<As—O>	1.8079	<As—O>	1.8092
Co—Co	2.81005(5)	Ni—Ni	2.8060(5)
∠O1 _b —As—O2 _i	96.76(3)×2	∠O1 _b —As—O2 _i	96.64(4)×2
∠O1 _b —As—O1 _b	99.03(4)	∠O1 _b —As—O1 _b	98.63(4)
∠As—O1 _b —As	124.09(6)	∠As—O1 _b —As	124.13(7)

Symmetry codes: (i) $y-1/2, x+1/2, -z+1/2$; (ii) $-x, -y+1, -z$; (iii) $-y+1/2, -x+1/2, z+1/2$; (iv) $-x, -y+1, z$; (v) $-x+1/2, y-1/2, -z$; (vi) $x, y, -z$.

Fourier transform infrared (FTIR) absorption spectra of the title compounds were recorded using a Bruker Tensor 27 FTIR spectrophotometer, equipped with mid-IR Globar light source and KBr beam splitter, attached to a Hyperion 2000 FTIR microscope with liquid nitrogen-cooled mid-IR, broad-band MCT detector. A total of 128 scans were accumulated between 4000 and 370 cm⁻¹ using the samples prepared as KBr pellets (KBr: MAs₂O₄ = 200:1).

2.4 Magnetic measurements

The magnetisation was measured with a QUANTUM DESIGN MPMS-XL-5 SQUID magnetometer. Zero-field-cooled (ZFC) and field-cooled (FC) runs were performed between room temperature and 2 K in a static magnetic field of 10 kOe, 1 kOe and 100 Oe. Isothermal magnetization curves were measured at several temperatures below and above the critical temperature.

3. Results and Discussion

3.1 Crystal structures

In the crystal structures of MAs₂O₄, the chains of edge-sharing MO₆ octahedra run parallel to the [001] direction, where the individual octahedra are orientated such that the apical, M—O1 bonds lie perpendicular to [001], and are directed towards the adjacent chain, which are further interconnected with the chains of corner sharing (AsO₃)³⁻ groups (Figs. 2 and 3).

The average Co—O and Ni—O bond lengths are 2.0795 and 2.046 Å. According to the formula $A_{oct} = 1/6 \sum [(d_i - d_m)/d_m]^2$ the bond-length distortions for the Co and Ni atoms amount to $1.11 \cdot 10^{-3}$ and $6.92 \cdot 10^{-4}$, respectively and indicate large distortions^{16,17}. These results compare well with the values compiled by Wildner¹⁸ for CoO₆ octahedra in accurately determined crystal structures, who found 672 Co—O bond lengths between 1.959 and 2.517 Å. The average <Co—O> bond lengths for 112 polyhedra are in the range of 2.054 to 2.182 Å; the overall mean value is 2.1115 Å.

The MO₆ octahedra are edge-linked to chains parallel to the 4-fold axis. The shared edges O2—O2ⁱ ($i = -x, -y+1, -z$) have lengths of 2.932(2) and 2.873(2) Å, for Co- and NiAs₂O₄, respectively. Due to this connection, the angular distortion is large: $\sigma_{oct}^2 = 1/11 \sum (\angle_i - 90)^\circ$ is 20.59 and 17.49 for the two CoO₆ and NiO₆ octahedra, respectively^{15,16}. The inter-transition metal separation distances, Co—Co and Ni—Ni along [001] are equal to the $c/2$ and amount 2.81005(5) and 2.8060(5) Å.

Arsenic is one-sided coordinated to three oxygen atoms and its coordination figure is represented by ψ -(AsO₃)³⁻ pyramids (ψ is a stereoactive lone pair of electrons), where the As atoms lies at the vertex and the oxygen atoms are at the basis of the pyramid. ψ -(AsO₃)³⁻ pyramids share corners thus forming chains also parallel to the 4-fold axis. Oxygen atoms of the pyramid basis lie parallel to the vertex and the oxygen atoms are at the basis of the pyramid. ψ -(AsO₃)³⁻ pyramids share corners thus forming chains also parallel to the 4-fold axis. Oxygen atoms of the pyramid basis lie parallel to the (110) plane, and the As-atoms alternate left and right from that plane (Fig. 3). The As—O bond lengths within the single chain are

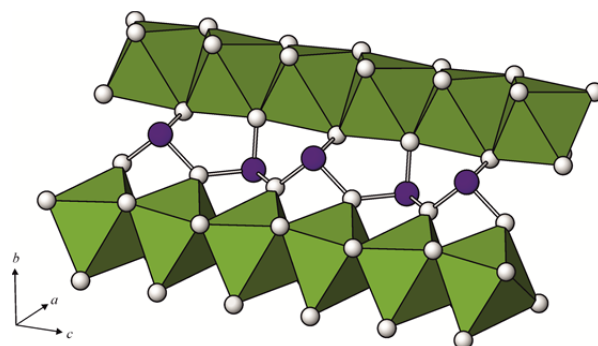


Figure 2 Part of the crystal structure of the tetragonal M²⁺X²⁺2O₄ compounds showing the connection of the MO₆ octahedral chains via trigonal ψ -(AsO₃)³⁻ pyramids.

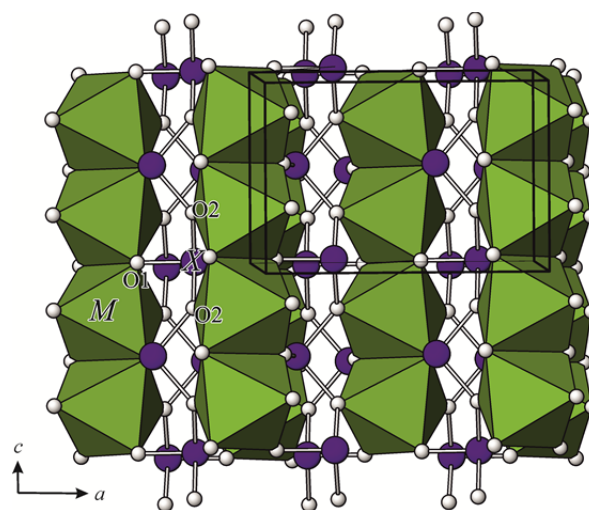


Figure 3 Perspective view of the crystal structure of the tetragonal M²⁺X²⁺2O₄ compounds.

significantly longer (1.8473(5) and 1.8501(6) Å, respectively) than the third As—O bond length (1.7292(11) and 1.7275(12) Å, respectively). As—O_{1b}—As angles within a single chain are 124.09(6)^o and 124.13(7)^o for CoAs₂O₄ and NiAs₂O₄, respectively and compare well with the As—O_b—As angles in other ‘chain’ arsenites [127.3(3)^o in CuAs₂O₄², from 123.3(5) to 125.1(3)^o in XAsO₂¹⁹, (X= Na, K, Rb), 125.1(14)^o in Cs₃As₅O₉¹⁸ and 121.3(5) and 122.3(5) in leelite, ZnAs₂O₄³.

Bond valence sum calculations²⁰ based on the room temperature data show the models to be compatible with the bonding requirements of Co²⁺ (2.10 v.u.), Ni²⁺ (2.08 v.u.) and As³⁺ (2.88/2.88 v.u.) O1 (2.24/2.26 v.u.), O2 (1.98/1.94 v.u.) for CoAs₂O₄ and NiAs₂O₄, respectively.

3.2 Vibrational spectra analysis

Spectroscopic data on arsenites that have been previously published are so far rather incomplete and not in good agreement with each other. However, the spectra assignments of CoAs₂O₄ and NiAs₂O₄ may be based on the single-crystal Raman study of synthetic trippkeite, CuAs₂O₄²¹ and AAsO₂¹⁹ (A = Na, K, and Rb). In the AAsO₂ compounds, where AsO₃ units are also interconnected to the chains (each unit possessing one terminal O and two bridging O atoms), the bands above 800 cm⁻¹ are observed in each spectrum. These bands were assigned to the vibration of terminal oxygen atoms. The bands at 810 and 780 cm⁻¹ in synthetic trippkeite are assigned to stretches of terminal O atoms and stretches of the bridging O atoms are assigned to bands at 657 and 496 cm⁻¹. Therefore the distinct frequency ranges in CoAs₂O₄ and NiAs₂O₄ may be assigned as follows:

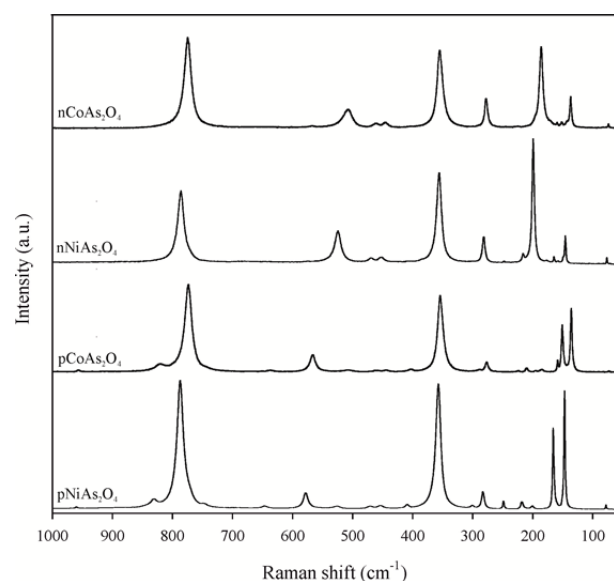
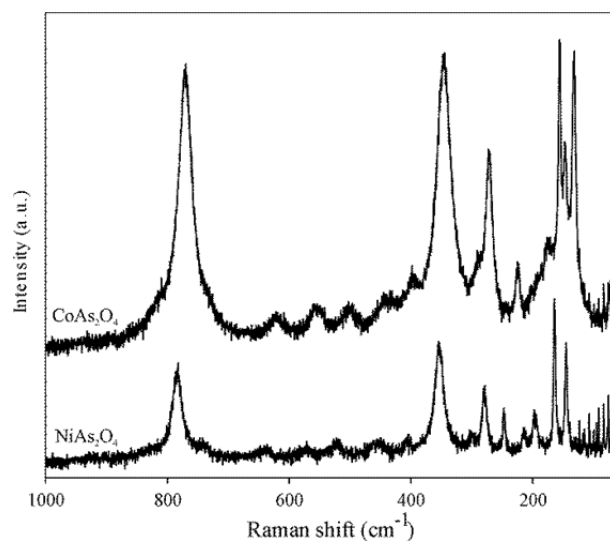


Figure 4 The single-crystal Raman spectra of CoAs₂O₄ and NiAs₂O₄ presented in two different orientations. p = elongation of the crystal is parallel to the laser beam, and n = elongation of the crystal is normal to the laser beam.

The Raman and infrared (IR) spectra of CoAs₂O₄ and NiAs₂O₄ are presented at the figures 4-6.

around 780 cm⁻¹ at 831 and 822 cm⁻¹ in NiAs₂O₄ and CoAs₂O₄,



respectively.

Figure 5 Raman spectra of the bulk CoAs₂O₄ and NiAs₂O₄ crystals.

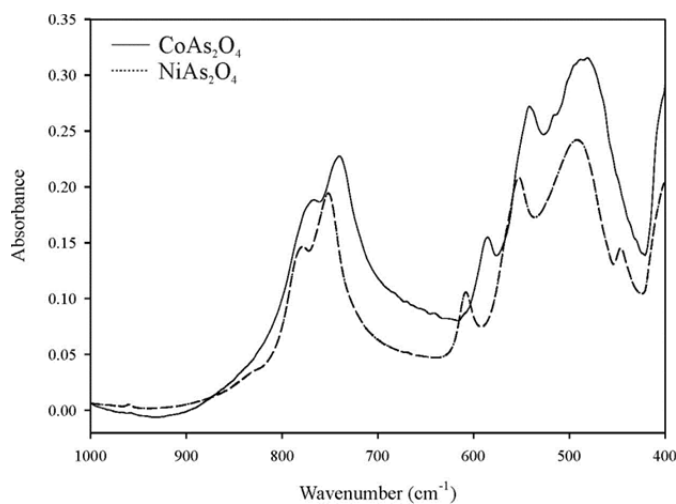


Figure 6 Infrared spectra of CoAs₂O₄ and NiAs₂O₄.

The Raman spectra of both title compounds were obtained aligning the laser beam parallel and normal to the longest axis of the single-crystal. The strong bands at 776 and 774 cm⁻¹ (778 cm⁻¹ in IR-spectrum and 783 cm⁻¹ in the Raman spectrum of the bulk) in NiAs₂O₄ and 787 and 780 cm⁻¹ (767 cm⁻¹ in IR-spectrum and 769 cm⁻¹ in the Raman spectrum of the bulk) in CoAs₂O₄ in parallel (*p*) and normal (*n*) orientation to the laser beam, respectively may be assigned to the symmetric As—O_{terminal} stretches, and the weak bands between 700 and 450 cm⁻¹ in both orientations and the bulk Raman spectra are assigned to the As—O_{bridging} stretches (strong bands at 533 and 494 cm⁻¹ and 540, 516, 486 cm⁻¹ in IR-spectrum of NiAs₂O₄ and CoAs₂O₄, respectively). In the *p* orientation of the Raman spectra, bands of very low intensity were observed at 960 and 958 cm⁻¹

(around 960 cm^{-1} in IR spectra) as well as a shoulder to the bands. These bands are attributed also to the symmetric As–O_{terminal} stretches. The very weak bands being seen only in *p* orientation at 747 and at the bulk spectrum (strong band at 753 cm^{-1}) and 646 cm^{-1} in NiAs₂O₄ and 638 cm^{-1} (strong band at 739 cm^{-1}) in CoAs₂O₄, respectively, may be attributed to the antisymmetric stretches. It is suggested that the (AsO₃)³⁻ group is the only tetrahedral oxyanion of the main group elements in which $\nu_s > \nu_{as}$ ²². The same is suggested for (As₂O₄)²⁻ group by Bencivenni and Gingerich²³. These authors noted that it was unusual for the vibrational spectroscopy of oxyanions. Further strong bands in the spectra of both arsenites are around 350 cm^{-1} (357 and 352 cm^{-1} in NiAs₂O₄ and 354 and 347 cm^{-1} in CoAs₂O₄) and are assigned to the ν_4 As₂O₄²⁻ bending modes and strong bands between 200 and 130 cm^{-1} . Below 300 cm^{-1} appear the various lattice modes of the compounds. The structure of Co- and NiAs₂O₄ consists of arrays of As–O–As–O–As chains. Two types of components are predicted based upon OAsO and AsOAs units. The bands between 300 and 200 cm^{-1} in the both compounds are assigned to the AsOAs linkages²⁴.

3.3 Magnetic properties

The magnetic properties of the NiAs₂O₄ and CoAs₂O₄ single crystals were investigated, since the presence of transition metals in chemical composition with unpaired *d* electrons indicates the non-diamagnetic ground state. All single crystals used for the magnetic measurements were studied by single-crystal X-ray diffraction techniques. The measurements showed the same primitive tetragonal unit cell, without additional non-indexed reflections. All single crystals have been probed in the constant magnetic field oriented with their *c*-axis parallel to the magnetic field ($H \parallel c$), while the crystals of CoAs₂O₄ has been measured also in $H \perp c$ orientation. The temperature dependence of the inverse molar magnetic susceptibility (measured at 10 kOe and displayed in Fig. 7) has a typical paramagnetic shape between room temperature and approximately 140 K, and can be described in the high temperature range (140–300 K) with the Curie–Weiss law: $\chi(T) = \chi_0 + C/(T-\theta)$, where χ_0 is the temperature-independent part of χ , i.e. diamagnetic contribution, *C* is the Curie constant, and θ is the Curie–Weiss temperature. From the slope of χ^{-1} vs *T* graph we obtain $p_{eff} = 3.3 \mu_B$ and Curie–Weiss temperature θ of approximately –40 K for NiAs₂O₄ as reported in Witteveen¹¹, while $p_{eff} = 5.6 \mu_B$ and $\theta \approx 75$ K for CoAs₂O₄ sample. The paramagnetic effective moments p_{eff} calculated from the Curie constant are in a close agreement with the literature data for Ni²⁺ cation (3.2 μ_B) and high spin Co²⁺ cation with large orbital contribution (6.5 μ_B)²⁵. Below 140 K the susceptibility of CoAs₂O₄ sample starts to deviate from paramagnetic (linear χ^{-1} vs. *T*) regime, while for NiAs₂O₄ the same occurs below 70 K. We also performed an equivalent analysis of inverse molar magnetic susceptibility measured under external field of 1 kOe, and obtained results are practically identical as for previously described measurement (Fig. S1 - Supporting Information).

Magnetic susceptibility measurements of NiAs₂O₄ under ZFC and FC conditions (Fig. 8a) show some unexpected results. At $T_N = 53$ K in high magnetic field of 10 kOe, the susceptibility shows behavior consistent with a transition to the antiferromagnetic ground state without splitting between ZFC and FC curves as already

reported²⁴. When the applied DC field is ten times lower, at the same temperature ZFC and FC curves start to diverge. Such divergence is highly enhanced when applied field was 100 Oe only. This first observed strong dependence of the transition at 55 K on magnetic field might be a consequence of two different superexchange interactions between Ni²⁺ ions: a positive and weaker one intrachain J_1 between magnetic moments in the chain, and a negative and stronger interchain interaction J_1 as proposed by Witteveen¹¹. The unexpected behaviour of ZFC–FC curves is detected at the temperature around 20 K, where the transition to the ferromagnetic state has been clearly observed. Finally, below 15 K ZFC–FC curves show a strong divergence.

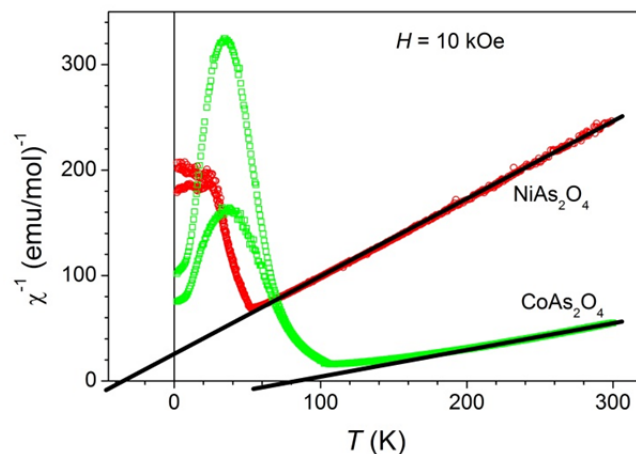


Figure 7 Temperature dependence of the inverse magnetic susceptibility for the studied NiAs₂O₄ and CoAs₂O₄ single crystals measured along crystal *c*-axis a DC field $H = 10$ kOe. The solid (black) lines are the best fit to the Curie–Weiss law at high temperatures

This second magnetic transition influences also the magnetization curves as only at 2 K where a small hysteresis with coercivity $H_c = 1.6$ kOe and remanent magnetization $M_r = 7.5 \cdot 10^{-3} \mu_B/\text{Ni}$ atom can be observed in M–H graph displayed in Figure 8b. *M*(*H*) curve measured at 50 K and 70 K is rather linear.

The phase transition from paramagnetic to magnetic ordered phase in CoAs₂O₄ occurs at higher temperature as in NiAs₂O₄. The positive Curie–Weiss temperature $\theta = 75$ K obtained from χ^{-1} vs. *T* plot suggests a ferromagnetic interaction between cobalt ions. Indeed, with decreasing temperature, the susceptibility measured in $H = 100$ Oe suddenly sharply increases at $T_c = 105.5$ K. The critical temperature T_c was defined from the fit $M \propto (1-T/T_c)^\beta$ as shown in inset in Fig. 9a. The obtained critical exponent $\beta = 0.34$ agrees with the theoretically calculated value for 3-D Ising system²⁶. The susceptibility at T_c and below behaves quite differently when measured in 1 kOe or 10 kOe instead of 100 Oe. It decreases below T_c as it is characteristic for antiferromagnetic transitions. The magnetisation curves *M* vs. *H* measured at several temperatures (Fig. 9b) also show this duality - ferromagnetic and antiferromagnetic behaviour. *M*(*H*) obtained at 2 K and 10 K exhibits an "S"-shaped curve for small magnetic fields that saturates at $\approx 0.01 \mu_B/(\text{Co ion})$ in a field of approx. 5 kOe. In larger magnetic fields magnetisation

increases linearly with the fields as expected for antiferromagnetically coupled magnetic moments.

The crystal structures of CoAs_2O_4 compound and the distribution of magnetic Co^{2+} ions in chains are similar to already reported NiAs_2O_4 ²² ($T_N = 53.5$ K), NiSb_2O_4 ²² ($T_N = 47$ K), MnSb_2O_4 ⁵ ($T_N = 55$ K), and CoSb_2O_4 ⁸ ($T_N = 79$ K). In the case of CoAs_2O_4 the magnetic ions Co^{2+} possess the largest magnetic moment among above mentioned compounds with the exception of CoSb_2O_4 where it is roughly the same. This may be the reason why the transition to magnetically ordered phase is shifted to a higher temperature for CoAs_2O_4 . Practically the same critical exponent as we obtained for CoAs_2O_4 ($\beta = 0.34$) was measured in MnSb_2O_4 ⁵ ($\beta = 0.36$) too. Having these similar structural and detected magnetic properties in mind, we propose the same - a canted antiferromagnetic structure of CoAs_2O_4 as described for MnSb_2O_4 ⁵. Such a structure is in agreement with a measured ferromagnetic response in a small magnetic field and prevailing antiferromagnetism when measured in magnetic field of 1 kOe or larger. In order to confirm the proposed magnetic structure neutron diffraction data are needed, for which there is not enough material at the moment.

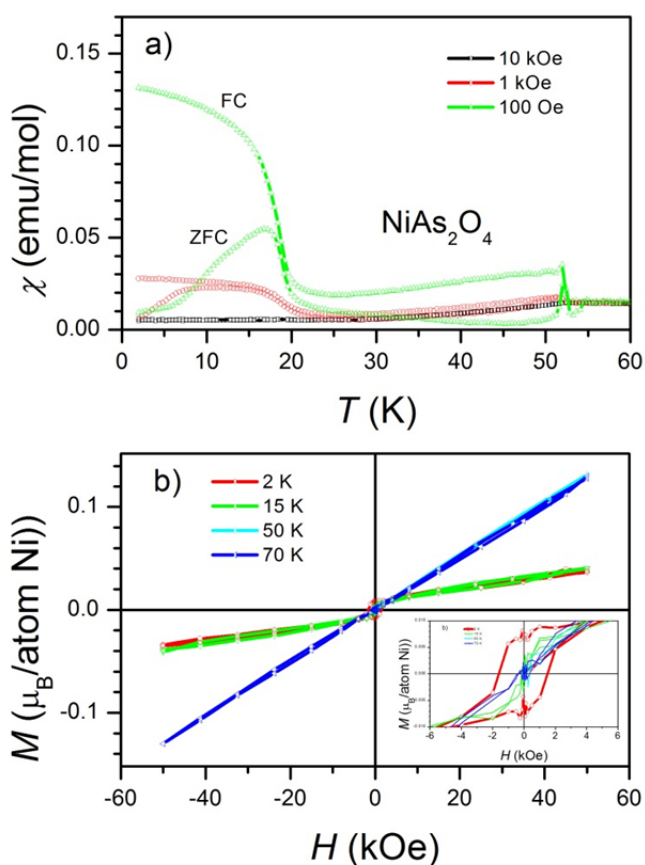


Figure 8(a) ZFC and FC molar magnetization versus temperature curves for NiAs_2O_4 measured in the various magnetic fields aligned along crystal c -axis. (b) Magnetization versus applied field aligned along crystal c axis for NiAs_2O_4 at 2, 15, 50 and 70 K.

Below 10 K a similar increase of the susceptibility in CoAs_2O_4 can be observed as already described for NiAs_2O_4 below 20 K. At the

moment we have no reliable explanation for these two increases of susceptibilities. Similar anomaly in the ZFC/FC susceptibility below about 20 K has been already detected for NiO nanoparticles and bulk materials²⁷⁻²⁹.

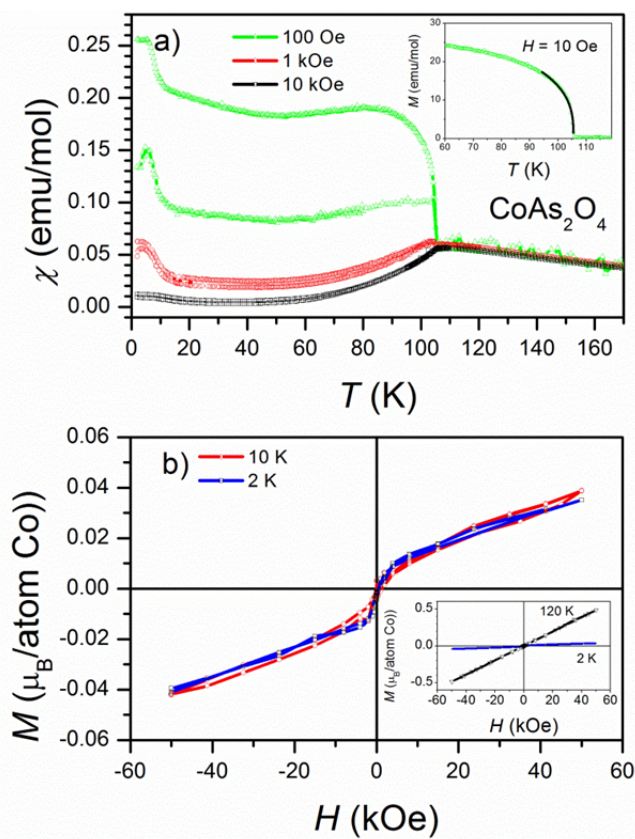


Figure 9 (a) ZFC and FC molar magnetization versus temperature curves for CoAs_2O_4 measured in the various magnetic fields aligned along crystal c -axis. Full line in inset is a fit $M \propto (1-T/T_c)^\beta$. (b) Magnetization versus applied field aligned along crystal c axis for CoAs_2O_4 at 2 K, 10 K, and 120 K (inset)

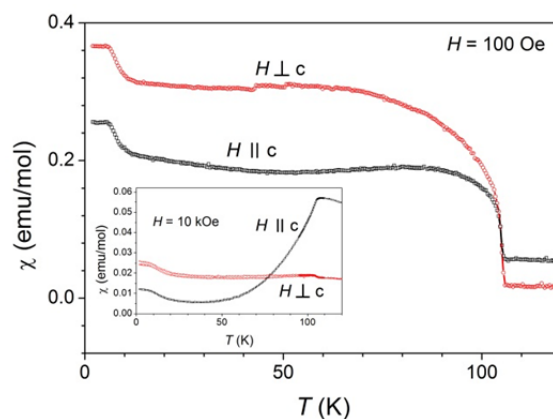


Figure 10 FC molar magnetization versus temperature curves for CoAs_2O_4 measured in 100 Oe in both alignment configurations (along crystal c -axis, and perpendicular to it). In the inset, it was shown a corresponding high-field measurement (10 kOe).

The anomaly was contributed to surface spin magnetism due to Ni^{2+} magnetic moments that are not coordinated in the same way as expected for the titled compound. We tentatively ascribe the measured anomalies at 20 K and 10 K in NiAs_2O_4 and CoAs_2O_4 , respectively, to the surface spins. In order to test this hypothesis much larger single crystals as we used in our research are needed.

The single-crystalline nature of investigated compounds points a further magnetic research into the possible magnetic anisotropy detection. In high magnetic field (1 T) the parallel and perpendicular susceptibilities, as shown in the inset of figure 10, are as expected for typical two-dimensional (layered) antiferromagnetic system as already described for $\text{BaNi}_2(\text{PO}_4)_2$ and $\text{Rb}_2\text{Co}_{0.7}\text{Mg}_{0.3}\text{F}_4$ ²⁶. While in small magnetic field of 100 Oe susceptibilities in both orientations of the sample increases below T_N . The increase is even larger for perpendicular orientation, in agreement with our hypothesis of canted magnetic moments from c-direction.

4. Conclusions

CoAs_2O_4 and NiAs_2O_4 were synthesised using low-temperature hydrothermal method, which resulted in beautiful, pure and homogeneous single crystals. In this manner, among isotypic $M^{2+}X^{3+}_2\text{O}_4$ compounds, the measuring of the magnetic properties using single-crystals was possible for the first time. Single-crystals also made us possible to extend our study of magnetic and vibrational properties to anisotropy measurements. MX_2O_4 compounds could be obtained by different synthesis routes (flux method, solid-state reaction, high-temperature hydrothermal method), but with the exception of CuAs_2O_4 , low-temperature hydrothermal method was used for the crystallization of suitable $M^{2+}X^{3+}_2\text{O}_4$ material for the first time.

The structurally characterised single crystal of NiAs_2O_4 , exhibit magnetic properties in accordance with the reported data. The magnetic susceptibility of NiAs_2O_4 at $T_N = 53$ K in high magnetic field of 10 kOe shows behaviour consistent with a transition to the antiferromagnetic ground state. However, at 20 K another transition to the ferromagnetic state has been clearly observed, which might be attributed to the uncompensated surface spins due to Ni^{2+} magnetic moments that are not coordinated in the same way as expected for the title compound. The SQUID measurement of the single crystal of CoAs_2O_4 reveals some subtle interplay between AFM and FM interactions in the system as evidenced as FM-like transition at 105.5 K in small magnetic field and AFM-like transition in 10 kOe and above. The transition at 105.5 K is, according to our knowledge, the highest critical temperature among all similar structures.

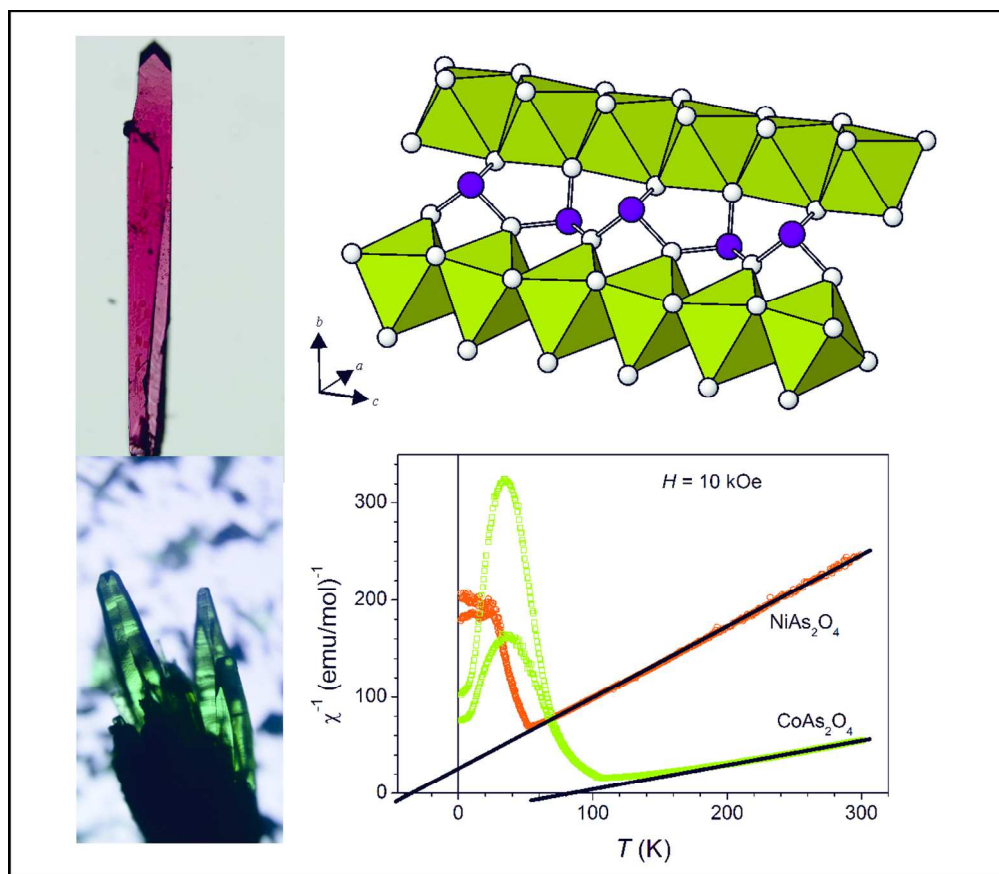
Acknowledgements

The authors gratefully acknowledge financial support from the Austrian Science Foundation (FWF) (Grant No. V203-N19), Austrian Student Exchange Service (ÖAD) and Austrian Ministry of Science (BM.W_f) (Bilateral cooperation project with Croatia 2014-15, Grant No. HR05/2014). The authors are thankful to Andreas Artač, M.Sc and Prof. Dr. Eugen Libowitzky for assisting during spectroscopic analysis.

References

- 1 S. Lösel and H. Hillebrecht, *Z. Anorg. Allg. Chem.*, 2008, **634**, 2299-2302.
- 2 F. Pertlik, *Tschermaks Min. Petr. Mitt.*, 1975, **22**, 211-217.
- 3 S. Ghose, P. K. S. Gupta and E. O. Schlemper, *Am. Mineral.*, 1987, **72**, 629-632.
- 4 C. Giroux-Maraine and G. Perez, *Revue Chim. Min.*, 1975, **12**, 427-432
- 5 H. Fjellvåg and A. Kjekshus, *Acta Chem. Scand.*, 1985, **A39**, 389-395.
- 6 R. Fischer and F. Pertlik, *Min. Petr. Mitt.*, 1975, **22**, 236-241.
- 7 J. R. Gavarri, R. Chater and J. Ziolkowski, *J. Solid State Chem.*, 1988, **73**, 305-316.
- 8 B. P. De Laune and C. Greaves, *J. Solid State Chem.*, 2012, **187**, 225-230.
- 9 E. G. Puebla, E. G. Ríos, A. Monge and I. Rasines, *Acta Crystallogr.*, 1982, **B38**, 2020-2022.
- 10 R. Chater, J.R. Gavarri and A.W. Hewat, *J. Solid State Chem.*, 1985 **60**, 78-86.
- 11 H. T. Witteveen, *Solid State Comm.*, 1971, **9**, 1313-1315.
- 12 F. Pertlik, *Monatsh. Chem.*, 1988, **119**, 4581-456.
- 13 SAINT, Bruker AXS Inc., 5465 East Cheryl Parkway, Madison, WI, 53711-5373, USA, 2000.
- 14 G. Sheldrick, *Acta Crystallogr.*, 2008, **A64**, 112-122.
- 15 L. J. Farrugia, *J. Appl. Cryst.*, 2012, **45**, 849-854.
- 16 K. Robinson, G. V. Gibbs and P. H. Ribbe, *Science*, 1971, **172**, 567-570.
- 17 M. E. Fleet, *Mineral. Mag.*, 1976, **40**, 531-533.
- 18 M. Wildner, *Zeit. Kristallogr.*, 1992, **202**, 51-70.
- 19 F. Emmerling and C. Röhr, *Z. Naturforsch.*, 2003, **58b**, 620-626.
- 20 N. E. Brese and M. O'Keefe, *Acta Crystallogr.*, 1988, **B47**, 192-197.
- 21 S. Bahfenne, L. Rintoul and R. L. Frost, *Am. Mineral.*, 2011, **96**: 888-894.
- 22 A. G. Nord, P. Kierkegaard, T. Stefanidis, and J. Baran, *Chem. Comm. University Stockholm*, 1988, **5**, 1-40.
- 23 L. Bencivenni and K. A. Gingerich, *J. Mol. Struct.*, 1983, **99**, 23-29.
- 24 R. L. Frost and S. Baffenne, *J. Raman Spec.*, 2010, **41**, 325-328.
- 25 N. W. Ascroft and N. D. Mermin, *Solid State Physics*, Saunders College Publishing USA, 1976, 657-658.
- 26 L. J. De Jongh, *Magnetic properties of layered transition metal compounds*, Kluwer Academic Publishers, Netherland, 1990
- 27 F. Bodker, M. F. Hansen, C. Bender Koch and S. J. Morup, *J. Magn. Magn. Mater.*, 2000, **221**, 32-36.
- 28 M. Jagodič, Z. Jagličić, A. Jelen, J.-B. Lee, Y.-M. Kim, H. J. Kim and J. Dolinšek, *J. Phys.: Condens. Matter*, 2009, **21**, 215302.
- 29 H. Shim, P. Dutta, M. S. Seehra and J. Bonevich, *Solid State Comm.*, 2008, **145**, 192-196.

The magnetic properties of the hydrothermally synthesised NiAs_2O_4 and CoAs_2O_4 single crystals were investigated, since the presence of transition metals in chemical composition with unpaired d electrons indicates the non-diamagnetic ground state. The unexpected behaviour of ZFC-FC curves of NiAs_2O_4 is detected at the temperature around 20 K, where the transition to the ferromagnetic state has been clearly observed.



112x97mm (300 x 300 DPI)